

# Molecular Weight Dependence of the Rotational Diffusivity of Rodlike Polymers in Concentrated Nematic Solutions

Aldo Acevedo,<sup>†</sup> Patricia M. Cotts,<sup>‡</sup> and Annette D. Shine<sup>\*,†</sup>

Department of Chemical Engineering, University of Delaware, Newark, Delaware 19716, and DuPont CR&D, Wilmington, Delaware 19880

Received July 6, 2004; Revised Manuscript Received May 26, 2005

**ABSTRACT:** The dynamics of rodlike polymer molecules in the nematic phase are mainly controlled by the rotational diffusivity,  $D_r$ , which is highly sensitive to molecular weight. However, few experimental determinations of  $D_r$  for polymer solutions at concentrations in the nematic phase have been made. We invoke Doi's theory of liquid crystalline polymer rheology to extract  $D_r$  from experimental measurements of the transverse Miesowicz viscosity,  $\eta_c$ , of nematic solutions. Transverse Miesowicz viscosities were measured for a series of poly(*n*-hexyl isocyanate) (PHIC) polymers at fixed dimensionless concentration ( $c/c^* = 1.25$ ) in *p*-xylene, by orienting the director with a high dc electric field. The rotational diffusivity of PHIC was found to be independent of shear rate and proportional to  $M_w^{-4.95 \pm 0.29}$ . This scaling is in excellent agreement with Doi's molecular theory, which predicts that  $D_r$  scales as  $M^{-5}$  at fixed  $c/c^*$ . The experimental values of  $D_r$  were compared with theoretical values calculated a priori from molecular dimensions and the solution concentration. The numerical constant  $\beta$  which multiplies Doi's predicted  $D_r$  was found to be of order  $10^1$  for the nematic PHIC solutions, in contrast with values of order  $10^3$  reported for semidilute solutions of rodlike molecules.

## 1. Introduction

The rotational dynamics of nematic solutions of rodlike polymers are of particular interest in areas such as processing of fibers<sup>1</sup> and thin films<sup>2</sup> and in electrorheological (ER) fluids,<sup>3</sup> where the orientation of the molecules controls the response and properties of the solution. Modeling of such problems usually involves fitting the rotational diffusivity to experimental data. For design purposes, a priori prediction of solution properties and rheological response from molecular inputs is desirable. The effect of fluid formulation parameters (e.g., molecular weight and concentration) on the rotational diffusivity of nematic solutions has not been extensively addressed, largely because experimental techniques, such as light scattering, are unsuitable in the nematic phase.<sup>4</sup> Hence, accurate theoretical predictions of the rotational diffusivity from molecular theory for nematic solutions would be especially useful.

Doi and Edwards<sup>5</sup> have described the dynamic behavior of interacting rodlike polymers through such a molecular-based tube model, which postulates that a rodlike macromolecule is confined to move inside a tube formed by its neighboring rods. The rotational diffusivity,  $D_r$ , quantifies the ability of the molecule to rotate around its center of mass. The rotational diffusivity in dilute solution,  $D_{r0}$ , can be estimated for rodlike polymers from hydrodynamics using molecular parameters as<sup>6</sup>

$$D_{r0} = \frac{3kT[\ln(L/d) - \gamma]}{\pi\eta_s L^3} \quad (1)$$

where  $d$  is the diameter and  $L$  the length of the rod,  $\eta_s$  is the solvent viscosity,  $\gamma$  is a correction factor for rod

**Table 1. Summary of Experimental Molecular Weight Scaling for Rotational Diffusivity of Rodlike Polymers**

polymer (solvent)	method	$D_r$ scaling	ref
Dilute: $D_r \propto M^{-3}f(M)^a$			
PHIC (toluene)	EB <sup>b</sup>	$M^{-2.90}$	24
PBIC (TCM) <sup>c</sup>	EB	$M^{-3} (M < 10^4)$	22
PBLG (DCE) <sup>d</sup>	DLS <sup>e</sup>	$M^{-2.7}$	13
Semidilute: $D_r \propto c^{-2}M^{-9}f(M)$			
PBLG (DCE)	DLS	$c^{-2}M^{-8}$	13
M-13 viruses	EB	$c^{-2}M^{-7.7}$	19
PBLG ( <i>m</i> -cresol)	EB	$c^{-1}M^{-7}$	15
Nematic: $D_r \propto (c/c^*)^{-2}M^{-5}f(M)$			
PBLG ( <i>m</i> -cresol)	rheo <sup>f</sup>	$M^{-5}$	27

<sup>a</sup>  $f(M) \equiv \ln M + \ln(b/M_0d) - \gamma$ . <sup>b</sup> Electric birefringence. <sup>c</sup> Tetrachloromethane. <sup>d</sup> 1,2-Dichloroethane. <sup>e</sup> Dynamic light scattering. <sup>f</sup> Rheology.

end effects, and  $kT$  is the product of the Boltzmann constant and the absolute temperature. A constant end effect correction factor ( $\gamma = 0.8$ ), calculated from point force approximations,<sup>7</sup> is often used. However, more recent predictions of the frictional forces on blunt cylinders<sup>8</sup> or cylinders capped with hemispheres<sup>9</sup> indicate that  $\gamma$  is a function of  $L/d$ . The Yoshizaki and Yamakawa approach<sup>9</sup> for a cylinder with oblate hemispherical end-caps having a semiaxis ratio of 0.63 predicts a change in  $\gamma$  from 0.33 to 0.57 when  $L/d$  increases from 10 to 60. For  $L/d > 60$ ,  $\gamma$  remains constant. The  $\ln(L/d) - \gamma$  term in eq 1 causes the  $L$  dependence of  $D_{r0}$  to be slightly less negative than the  $-3$  power. Table 1 shows that the predicted length scaling of  $L^{-3}[\ln(L/d) - \gamma]$  for  $D_{r0}$  has been verified experimentally.

Above a certain critical concentration the molecules tend to align toward the same average direction, and a liquid crystalline phase is observed. In this regime the rotational diffusivity is dependent on the orientation of an individual molecule and its local environment. Doi<sup>10</sup> suggested an orientation-independent averaged diffu-

<sup>†</sup> University of Delaware.

<sup>‡</sup> DuPont CR&D.

\* To whom correspondence should be addressed: Ph (302) 831-2010; Fax (302) 831-1048; e-mail shine@che.udel.edu.

sivity, which eliminates the extensive mathematical analysis otherwise required and is given for concentrated nematic solutions as

$$D_r = \frac{\beta D_{r0}}{c^2 L^6 R^2} \quad (2)$$

where  $\beta$  is a numerical factor and  $c$  is the number concentration (molecules per volume). The factor  $R$  accounts for the effect of tube dilation and is given by

$$R = \frac{4}{\pi} \int du du' f(u) f(u') |u \times u'| \quad (3)$$

where  $u$  and  $u'$  are unit vectors parallel to a test rod and its neighboring rods, respectively, and  $f(u)$  is the molecular orientation distribution function. When polymer molecules orient in the same direction, the average diameter of the confining tube becomes larger, so the rotational diffusivity increases. The integral term  $R$  is thus related to the order parameter,  $S$ , of the nematic solution.

Substituting eq 1 into eq 2 yields

$$D_r = \frac{\beta \pi kT}{\eta_s R^2 c^2} \frac{[\ln(L/d) - \gamma]}{L^9} \quad (4)$$

Equation 4 predicts an inverse square dependence of the rotational diffusivity in the nematic regime on number concentration ( $D_r \propto c^{-2}$ ). At a constant value of  $c$ , the rotational diffusivity varies with molecular length as  $L^{-9}(\ln(L/d) - \gamma)$ . For rodlike polymers the molecular weight ( $M$ ) is proportional to  $L$ , hence, in terms of molecular weight, the rotational diffusivity from eq 4 is expressed as

$$D_r = \frac{3\beta kTM_0^9 [\ln(M) + \ln(b/M_0d) - \gamma]}{\pi \eta_s c^2 b^9 M^9 R^2} \quad (5)$$

where  $b$  and  $M_0$  are the projection length and molecular weight of a monomer unit. The integral term  $R$  is actually a function of the dimensionless concentration  $C = c/c^*$ , where  $c^*$  is the number concentration where the isotropic phase becomes unstable.  $c^*$  can be inferred from either experimental measurements of phase transitions or predicted with the aid of theory. Onsager's theory<sup>11</sup> for the phase behavior of perfectly rigid rods predicts the relation

$$c^* = 16/\pi dL^2 \quad (6)$$

Substituting eq 6 into eq 5 shows that, for fixed  $c/c^*$ , the rotational diffusivity varies with molecular length as  $M^{-5}f(M)$ , where  $f(M) \equiv \ln M + \ln(b/M_0d) - \gamma$ , viz.

$$D_r = \frac{3\beta \pi d^2 kTM_0^5}{256 \eta_s R^2 b^5} \left(\frac{c^*}{c}\right)^2 \frac{\ln(M) + \ln(b/M_0d) - \gamma}{M^5} \quad (7)$$

Equations 5 and 7 demonstrate that the rotational diffusivity can be calculated directly from molecular parameters, provided that the numerical value of  $\beta$  is known and that an algorithm exists for estimating  $R$ .

Initially, the numerical factor  $\beta$  was expected to be of order unity;<sup>5</sup> however, larger values have been reported from fits to experimental data. Chow and co-workers reported values of  $\beta$  of the order of  $10^6$  from

rheoptical experiments of semidilute collagen solutions,<sup>12</sup> while values of  $O(10^3)$  have been reported for semidilute solutions of poly( $\gamma$ -benzyl L-glutamate) (PBLG) in 1,2-dichloroethane (DCE).<sup>13</sup> In these cases, the increase in  $\beta$  was attributed to flexibility, which decreases the effective rod length. Nevertheless, Teraoka and co-workers<sup>14</sup> calculated a value of  $\beta = 1320$  from computer simulation of tube statistics for perfectly rigid rods in semidilute solutions. Their main assumption was that the rodlike polymer does not have to move a distance  $L$  to disengage from its surrounding tube in order to rotate. Their result was found to be consistent with the experimental results of Mori et al.<sup>15</sup> for PBLG in *m*-cresol.

Experimental techniques such as dynamic light scattering,<sup>13,16–18</sup> electric birefringence,<sup>15,19–24</sup> and optical rheometry (flow birefringence)<sup>12,25,26</sup> have been used to measure the rotational diffusivity or the rotational relaxation time ( $\tau = 1/6D_r$ ) in the dilute and semidilute regimes; scaling results are summarized in Table 1. In dilute solutions,  $D_{r0}$  scales with a power slightly less negative than  $-3$  as predicted by eq 1. In the semidilute regime, eq 2 applies for  $R = 1$  (no preferred orientation). Good agreement has been found with the predicted concentration and molecular weight scaling and experimental results in this regime (Table 1). Molecular weight studies usually include molecules from both the rigid and semiflexible regions, so the slight discrepancy toward lower values of the exponent dependencies are often attributed to chain flexibility.<sup>22,25</sup> Experiments in concentrated liquid crystalline solutions have been limited to relating rheological properties to characteristic molecular relaxation times and thus to the rotational diffusivity. Gleeson and co-workers<sup>27</sup> found experimentally for the lyotrope PBLG in *m*-cresol that the shear rate at which the first normal stress difference,  $N_1$ , reaches its positive maximum,  $\dot{\gamma}_{\max}$ , scales as  $M^{-5}$  for molecular weights ranging from 86 to 238 kDa at a fixed value of  $c/c_{IN} \sim 1.12$ , where  $c_{IN}$  is the concentration for the inception of the nematic phase. The molecular relaxation time is proportional to  $De/\dot{\gamma}_{\max}$ ,<sup>28</sup> where  $De$  is a constant Deborah number independent of molecular weight. Therefore, the rotational diffusivity is proportional to  $\dot{\gamma}_{\max}$  and consequently to  $M^{-5}$ .

In this paper, Doi's theory of liquid crystalline polymer rheology is used to extract  $D_r$  of nematic solutions from experimental measurements of the transverse Miesowicz viscosity,  $\eta_c$ . Transverse Miesowicz viscosities were measured for a series of poly(*n*-hexyl isocyanate) (PHIC) polymers at fixed dimensionless concentration ( $c/c^* = 1.25$ ) in *p*-xylene, by orienting the director with a high dc electric field. The nematic potential,  $U$ , is only a function of the dimensionless concentration,  $c/c^*$ ; thus, a comparable nematic state was achieved by fixing  $c/c^*$ . PHIC is a well-studied model of rodlike polymers with a large permanent dipole moment along the main rod axis, making it ideal for ER studies. Scaling arguments for the effect of molecular weight and shear rate on the Miesowicz viscosity,  $\eta_c$ , and the rotational diffusivity are tested. Finally, the experimental rotational diffusivity is compared with a priori predictions from eq 7 using molecular parameters for PHIC.

## 2. Background

After development of the molecular theory for the rheology of liquid crystalline polymers by Doi, other authors have shown the equivalence between the phe-

nomenological Ericksen–Leslie–Parodi (ELP) theory and the Doi molecular theory.<sup>29–31</sup> The Leslie coefficients can thus be expressed as functions of molecular parameters, such as concentration and rotational diffusivity.

The macroscopically measurable Miesowicz viscosities,  $\eta_a$ ,  $\eta_b$ , and  $\eta_c$ , are the liquid crystal viscosities when the director (average orientation of the molecules) is oriented in the vorticity, flow, and velocity gradient directions, respectively. Because the Miesowicz viscosities are linear combinations of the Leslie coefficients, they too can be related to molecular and solution parameters. The nematic director can be oriented through the application of an external electric or magnetic field.<sup>32</sup> Lee and co-workers extracted the rotational diffusivity of poly(*p*-phenylene terephthalamide) (PPTA) in sulfuric acid solutions from measurements of  $\eta_b$  in Poiseuille flow under an electric field.<sup>33</sup> In this work, we have adopted a similar procedure to extract  $D_r$  from  $\eta_c$ , but without the shortcomings of the decoupling approximation used by Marrucci.<sup>29</sup>

Steady-state ER characterization of simple shear flows with an applied electric field perpendicular to the shear direction of nematic PHIC solutions have shown that the viscosity increases sigmoidally above a threshold electric field until it reaches a plateau or maximum value.<sup>34</sup> Conoscopy experiments have demonstrated that the plateau viscosity corresponds to the Miesowicz viscosity,  $\eta_c$ , where the director is oriented parallel to the velocity gradient and the electric field.<sup>3</sup> Consequently, an experimentally measurable quantity, the plateau viscosity, can be used to study the effects of molecular parameters such as concentration and molecular weight on the rotational diffusivity,  $D_r$ .

The Miesowicz viscosity,  $\eta_c$ , is expressed in terms of the Leslie coefficients ( $\alpha_i$ 's) as

$$\eta_c = \frac{1}{2}(-\alpha_2 + \alpha_4 + \alpha_5) \quad (8)$$

Kuzuu and Doi<sup>35</sup> obtained expressions for the Leslie coefficients in terms of molecular parameters without the use of the decoupling approximation. The relevant coefficients in eq 8 are given as

$$\alpha_2/\eta^* = -5C^3PR^2(1 + \lambda^{-1})S_2 \quad (9a)$$

$$\alpha_4/\eta^* = \frac{2}{7}C^3P^2R^2(7 - 5S_2 - 2S_4) \quad (9b)$$

$$\alpha_5/\eta^* = 5C^3R^2P\left(\frac{1}{7}P(3S_2 + 4S_4) + S_2\right) \quad (9c)$$

where  $S_2$  and  $S_4$  are the second and fourth equilibrium order parameters, respectively,  $\lambda$  is the “tumbling” parameter,  $R$  is the tube dilation factor from eq 3, and  $P$  is a shape factor. For rodlike polymers with large  $L/d$ ,  $P$  approaches unity.<sup>36</sup> Equations 8 and 9 are scaled with respect to  $\eta^*$ , the viscosity of the isotropic phase at  $c^*$ , which is given as

$$\eta^* = \frac{c^*kT}{10D_r^*} \quad (10)$$

where  $D_r^*$  is the rotational diffusivity of the isotropic phase at  $c^*$ . A perturbation method was used by Kuzuu and Doi<sup>30</sup> to expand  $S_2$ ,  $S_4$ , and  $R$  as power series of  $C$  ( $= c/c^*$ ), yielding

$$S_2 = 1 - 0.1473C^{-2} - 3.344 \times 10^{-2}C^{-4} - 1.49 \times 10^{-2}C^{-6} \quad (11a)$$

$$S_4 = 1 - 0.4909C^{-2} - 2.713 \times 10^{-2}C^{-4} - 1.56 \times 10^{-2}C^{-6} \quad (11b)$$

$$R = \frac{2.25676}{B^{0.5}} - \frac{2.116}{B^{1.5}} + \frac{0.474}{B^{2.5}} \quad (11c)$$

$$B = 20.371C^2 - 5.626 - 1.06C^{-2} \quad (11d)$$

A simple approximation for the tumbling parameter was proposed by Archer and Larson<sup>37</sup> in terms of the form factor and the order parameters as

$$\lambda = P \frac{5S_2 + 16S_4 + 14}{35S_2} \quad (12)$$

Equations 8–12 predict that the ratio  $\eta_c/\eta^*$  is only a function of  $c/c^*$ . Consequently, the Miesowicz viscosity follows a similar scaling with molecular weight at a fixed  $c/c^*$  as the viscosity of the isotropic phase at  $c^*$ . By substituting eqs 6 and 7 into eq 10, it can be shown that the Miesowicz viscosity scales with molecular weight as

$$\eta_c \propto \eta^* \propto M^3 f(M)^{-1} \quad (13)$$

Doi theory also predicts a similar dependence of  $M^3 f(M)^{-1}$  for the zero-field viscosity.<sup>6</sup>

We have determined the rotational diffusivity from the experimentally measured Miesowicz viscosity,  $\eta_c$ , as follows: for a known  $C$ , the parameters  $R$ ,  $S_2$ ,  $S_4$ , and  $\lambda$  were calculated from eqs 11 and 12. Then, eqs 8 and 9 were solved for  $\eta^*$ . The rotational diffusivity at  $c^*$  was calculated from eq 10. Since from eq 2  $D_r \propto c^{-2}R^{-2}$ , taking  $R = 1$  in the isotropic phase yields

$$D_r = D_r^* C^{-2} R^{-2} \quad (14)$$

The rotational diffusivity was calculated as described above at various concentrations corresponding to  $c/c^*$  from 1.0 to 1.14 from the plateau viscosity for solutions of PHIC of  $M_v = 100$  kDa in *p*-xylene reported by Tse and Shine.<sup>3</sup> Results are shown in Figure 1, where they are compared to the rotational diffusivity reported by the same authors from fittings of steady-state electroviscosity to their ER model.<sup>38</sup> The calculated  $D_r$  is observed to be proportional to the  $-2.66 \pm 0.33$  power of concentration, similar to that observed by the same authors and in near agreement with predictions of Doi's theory. Only small (<5%) differences are seen between the two estimation procedures; we believe the current method is preferable for use since it does not require numerical simulation.

### 3. Experimental Section

PHIC was synthesized by an organotitanium(IV)-catalyzed living polymerization reaction.<sup>39</sup> This polymerization is both living, which leads to a monodisperse molecular weight distribution, and reversible, which, if allowed to proceed to equilibrium, results in the most probable molecular weight distribution with a polydispersity index of 2.0.<sup>40</sup> The catalyst used was  $\text{TiCl}_3\text{OCH}_2\text{CF}_3$  (kindly synthesized by Dr. David Thorn, DuPont). In a drybox with a nitrogen atmosphere, a catalyst solution of approximately 1 g in 30 mL of toluene was



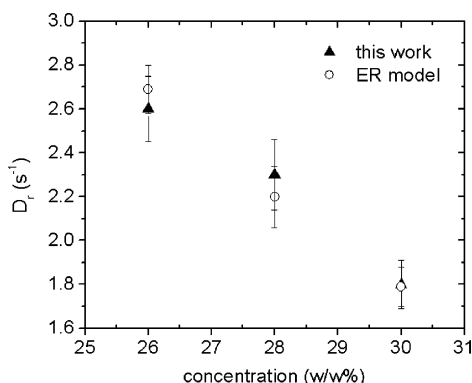


**Figure 1.** Rotational diffusivity calculated from plateau viscosities reported by Tse and Shine (2000) ( $\blacktriangle$ ) and comparison with reported results from the electrorheological model of the same authors ( $\circ$ ) for a  $M_v = 100$  kDa PHIC in nematic *p*-xylene solutions.

prepared. In a 25 mL flask, catalyst solution and *n*-hexyl isocyanate (99%, Acros Organics) were mixed at room temperature, stirring continuously, at different catalyst-to-monomer ratios. The reaction mixture turned an orange color, and its viscosity increased substantially as the reaction progressed. At the appropriate time, generally 3–24 h after initiation, the reaction was transferred to a bigger flask and terminated by the addition of an excess of acetic anhydride (99%, Aldrich & Alfa Aesar) in a 1:10 volume ratio. Acetic anhydride quenches the active end of the chain, halting both the propagation and depropagation steps.<sup>41</sup> The quenched mixture was left to react for at least 4 h, after which 50 mL of toluene was added to the mixture. The polymer mixture was precipitated into methanol in a 1:4 volume ratio and recovered by filtration. To eliminate uncapped chains, the polymer was redissolved in 200 mL of toluene and left at room temperature for at least 24 h to promote depolymerization. Following subsequent methanol precipitation, the filtered polymer was dried in vacuo at 40 °C for at least 4 h. All solvents used in solutions were incubated with molecular sieves at least 1 week prior to use in order to eliminate moisture and were bubbled with nitrogen before use. Recovered polymer ranged from 2.5 to 6.0 g, yielding a monomer-to-polymer conversion that was always less than 50%; low conversion was desirable to minimize polydispersity.

Intrinsic viscosity was measured in toluene at 25 °C. The viscosity-average molecular weight ( $M_v$ ) was calculated using the Mark–Houwink constants of  $K = 2.99 \times 10^{-6}$  and  $a = 1.2$ .<sup>42</sup> Another PHIC sample was obtained from Polysciences, Inc. (lot #452029). The commercial sample was cleaned following the procedures described above prior to use to eliminate side products (primarily trimers) of the synthesis procedure. An additional sample from our laboratory inventory was also used; synthesis details have been given elsewhere.<sup>3</sup> The molecular weight distributions of all samples were obtained in a tandem SEC/LS apparatus using a Waters Alliance 2690 liquid chromatograph connected to a Wyatt Dawn EOS multiangle light scattering spectrometer and a Viscotek dual detector (refractive index and differential viscosity). The  $M_v$  measured by the Viscotek detector agreed with the intrinsic viscosity measurements in toluene to within a standard deviation of  $\pm 10\%$ , except for the Polysciences sample where the standard deviation was  $\pm 15\%$ .

Results for molecular weight averages and polydispersities of the synthesized PHIC are summarized in Table 2. Determination of  $M_n$  can be problematic in SEC light scattering due to insufficient scattering at the lowest molecular weight portion of the distribution. This was addressed by fitting the calibration curve of  $M$  as a function of elution volume in the region where light scattering was sufficient and extending this fit to encompass the low molecular weight region. The molecular weight averages,  $M_n$ ,  $M_w$ , and so forth, were then calculated as is usually done for SEC. In the case of the PHIC

**Table 2.** Molecular Weight Characterization and Phase Behavior of the Synthesized PHIC

$M_v$ (kDa) <sup>a</sup>	$M_n$ (kDa)	$M_w$ (kDa)	PDI	$c_{IN}$ (wt %)	$c_{nem}$ (wt %)
29.3	13.2	22.5	1.70	28.3	37.2
41.6	21.0	29.7	1.41	25.3	33.6
50.6	21.5	33.6	1.57	23.5	34.0
72.2	31.3	49.8	1.59	23.1	34.5
122.3 <sup>b</sup>	54.7	99.2	1.81	21.2	29.0
149.0 <sup>c</sup>	65.1	109.6	1.68	21.1	

<sup>a</sup> Average values from intrinsic viscosity in toluene and Viscotek detector. <sup>b</sup> Sample obtained from Polysciences, Inc. <sup>c</sup> Sample from laboratory inventory.

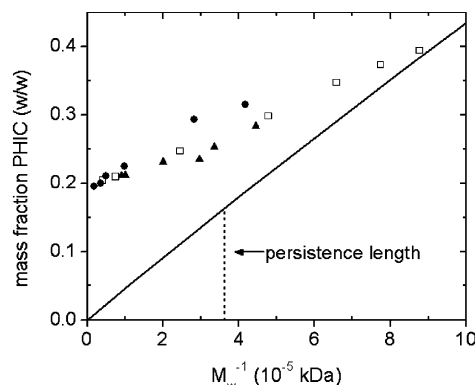


**Figure 2.** Molecular weight dependence of the isotropic-to-nematic (IN) phase transition concentration of PHIC: ( $\blacktriangle$ ) in *p*-xylene, present work; ( $\square$ ) in toluene at 25 °C, Itou and Teramoto;<sup>44</sup> ( $\bullet$ ) in toluene at 20 °C, Conio et al.;<sup>43</sup> (—) predictions from Onsager's rigid-rod theory.<sup>11</sup>

series, the data obtained for the lower molecular weight samples was also consistent with this extrapolation. The polydispersity index ( $PDI = M_w/M_n$ ) ranged from 1.41 to 1.81. The persistence length of PHIC in toluene at 25 °C is 37 nm; thus, the samples used in this work range from about 0.81 to 3.96 persistence lengths.

The liquid crystalline phase behavior of solutions of PHIC in *p*-xylene was observed with an optical microscope (Nikon Optiphot-2) under crossed polarizers. The concentration of the isotropic-to-nematic transition ( $c_{IN}$ ) was taken as the point where the first liquid crystalline regions became visible and was determined to within 0.2 wt %. Similarly, the concentration of the biphasic-to-fully nematic transition ( $c_{nem}$ ) was taken as the point where the sample became fully birefringent. Greater accuracy was achieved in the determination of  $c_{IN}$ , making it more suitable as a reference point, than  $c_{nem}$ , where the high light intensity made it difficult to identify isotropic inclusions visually. Phase behavior results are included in Table 2.

Figure 2 shows the results of the isotropic-to-nematic phase transition of PHIC in *p*-xylene at room temperature ( $\sim 23$  °C). Reported values for PHIC in toluene<sup>43,44</sup> and the predictions for the phase transition of perfectly rigid rods based on Onsager's theory<sup>11</sup> have been plotted for comparison. The chain dimensions of PHIC in toluene<sup>42</sup> were used for the Onsager predictions, specifically,  $b = 0.17$  nm and  $d = 1.6$  nm. The concentration of the IN transition decreased as molecular weight increased until it approached a constant value as  $1/M$  approached zero. However, rigid-rod theory predicts an intercept of zero. From phase behavior data, the critical concentration,  $c^*$ , above which the isotropic phase becomes unstable was estimated as 1.198 times  $c_{IN}$  on the basis of Onsager's theory. A constant value of  $c/c^*$  of 1.25 was used in all rheological characterization to keep the nematic potential fixed.

Electrorheological characterization was performed on a Rheometrics ARES strain controlled rheometer using stainless steel parallel plates, where a dc electric field was provided by a TreK-610C high-voltage supply. Parallel plate geometry provided a constant electric field throughout the sample. All

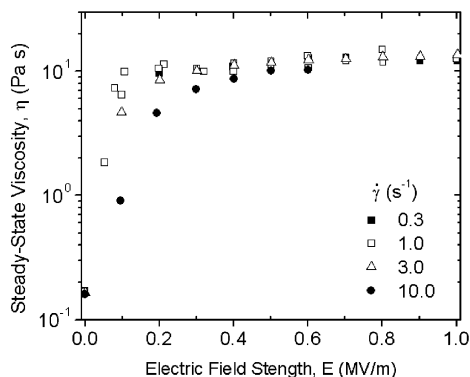


**Figure 3.** Electroviscosity at various shear rates for PHIC ( $M_w = 22.5$  kDa) in *p*-xylene solution at  $c/c^* = 1.25$  and  $25^\circ\text{C}$ . Symbols are for  $\dot{\gamma} = 0.3$  (■),  $1$  (□),  $3$  (△), and  $10$   $\text{s}^{-1}$  (●).

rheological measurements were performed at a constant temperature of  $25^\circ\text{C}$ , using a Peltier plate temperature control unit as the lower fixture. The plates had either a 50 or 25 mm diameter, with a gap of 0.4 or 0.5 mm; no effect of geometry on results was observed. The fixtures were enclosed in an environmental chamber equipped with humidity pads soaked in *p*-xylene to retard solvent evaporation.

The samples were allowed to relax for 10–15 min after initial loading. Following this, a constant shear rate deformation was suddenly initiated, with a simultaneous change of the electric field to the desired dc voltage. The field was held constant until steady state was achieved. Stepwise changes in the applied voltage were used to examine the electrorheology of the solution and record the steady-state viscosity at constant shear rates. No difference between steady-state measurements following step-up or step-down of the applied electric field was observed. Edge shear rates ranging from 0.3 to  $10\text{ s}^{-1}$  were used, with dc electric field strengths ranging from 0 to 1.2 MV/m. For  $M_w \leq 49.8$  kDa, these edge shear rates were always in the Newtonian region of the zero-viscosity curve; however, the higher molecular weights showed shear thinning behavior at shear rates above  $3\text{ s}^{-1}$ . Data from shear rates in the shear thinning regime were not analyzed because these conditions required a higher electric field to orient the nematic phase than was available with the ARES instrument. The electric field was limited by the need to avoid overloading the normal stress transducer, since large attractive stresses are generated between the plates.

#### 4. Results

The steady-state electroviscosity of a  $M_w = 22.5$  kDa PHIC solution as a function of electric field strength for shear rates ranging from 0.1 to  $10\text{ s}^{-1}$  is shown in Figure 3. At a fixed shear rate, the electroviscosity is seen to increase with increasing electric field until a maximum plateau viscosity is reached. This maximum viscosity was 2 orders of magnitude larger than the viscosity in the absence of the electric field. Each shear rate curve reached the same plateau viscosity, which corresponds to the transverse Miesowicz viscosity,  $\eta_c$ .<sup>3</sup> However, the plateau was reached at lower values of the applied field for lower shear rates. The steady-state electroviscosity of PHIC solutions at a constant shear rate of  $1\text{ s}^{-1}$  and  $c/c^* = 1.25$  for different  $M_w$  samples is shown in Figure 4. The Miesowicz viscosity increased significantly with increasing molecular weight, although plateau values were not achieved at this shear rate for the higher molecular weight samples.

Plateau viscosities were estimated for all molecular weights and shear rates within the Newtonian plateau by extrapolating high field data to  $1/E \rightarrow 0$ . This extrapolation compensated for equipment limitations preventing the use of higher electric fields and for the

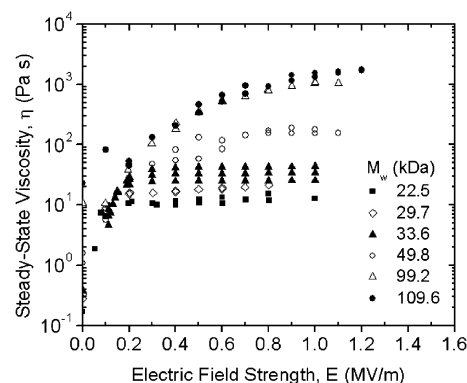


**Figure 4.** Molecular weight effect on the steady-state electroviscosity of nematic PHIC/*p*-xylene solutions at  $\dot{\gamma} = 1\text{ s}^{-1}$  and  $c/c^* = 1.25$ . Symbols correspond to  $M_w = 22.5$  (■),  $29.7$  (◇),  $33.6$  (▲),  $49.8$  (○),  $99.2$  (△), and  $109.6$  kDa (●).

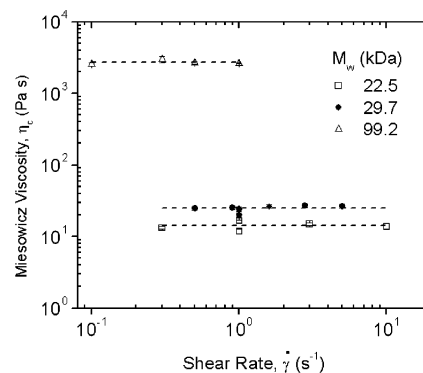


**Figure 5.** Effect of shear rate on the Miesowicz viscosity,  $\eta_c$ , from electrorheological data for  $M_w$  ranging from 22.5 to 99.2 kDa at a  $c/c^* = 1.25$ . Lines correspond to average values.

slight increase in viscosity at high fields due to a slight increase in the order parameter. In all parameter fitting and averaging procedures, data points were weighted by the inverse square of the propagated standard error. For plateau viscosity estimation, the standard error at each molecular weight was taken to be the same relative error as that determined from the standard deviation of individual reproducibility measurements. Figure 5 demonstrates that, for each molecular weight, the Miesowicz viscosities were independent of shear rate to within experimental error. The results are consistent with previous reports of the electrorheology of a 30 wt % PHIC ( $M_v = 100$  kDa) solution.<sup>3</sup>

#### 5. Discussion

Table 3 lists the Miesowicz viscosity and the zero-field shear viscosity of the PHIC samples as a function of molecular weight; reported values are weighted averages for all shear rates studied. Since  $b$ ,  $M_0$ , and  $d$  are known molecular parameters, and  $\gamma$  can be calculated, the value of  $f(M)$  can be calculated for each of our samples. We used a monomer molecular weight ( $M_0$ ) of  $127\text{ g/mol}$ , the chain dimensions for PHIC in toluene,  $b = 0.17\text{ nm}$  and  $d = 1.6\text{ nm}$ , and used the procedure of Yoshizaki and Yamakawa<sup>9</sup> for oblate hemispheroidal end caps having a semiaxis ratio of 0.63 to determine values for  $\gamma$ . Calculated values of  $\gamma$  for our PHIC samples with axial ratios  $L/d$  between 18.8 and 91.6 are also shown in Table 3. To test the data against the predictions of Doi's theory for rigid-rod-like polymers, shown in eq 13, the viscosity data were multiplied by  $f(M)$  for the linearized plot in Figure 6. At higher

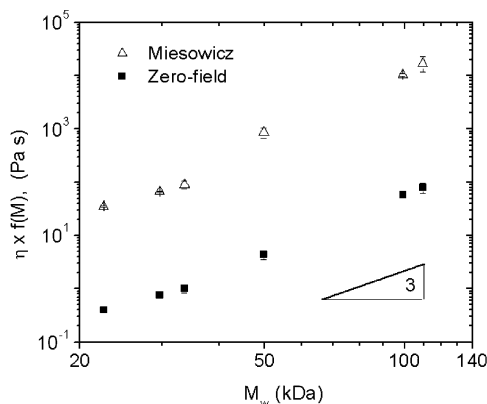
**Table 3. Experimentally Measured Zero-Field Viscosity ( $\eta_{E=0}$ ), Miesowicz Viscosity ( $\eta_c$ ), and Calculated  $\gamma$ ,  $\eta^*$ , and Rotational Diffusivities from Eqs 8–14 for  $M_w = 22.5$  to 109.6 kDa**

$M_w$ (kDa)	$\eta_{E=0}$ (Pa s)	$\eta_c$ (Pa s)	$\gamma$	$\eta^*$ (Pa s)	$D_r$ ( $s^{-1}$ )
22.5	$0.16 \pm 0.01$	$14.2 \pm 0.4$	0.47	$4.396 \pm 0.124$	$2531 \pm 62$
29.7	$0.28 \pm 0.02$	$24.8 \pm 0.5$	0.51	$7.678 \pm 0.155$	$981 \pm 21$
33.6	$0.36 \pm 0.06$	$32.3 \pm 5.4$	0.53	$10.00 \pm 1.67$	$619 \pm 103$
49.8	$1.38 \pm 0.26$	$272 \pm 58$	0.56	$84.21 \pm 17.96$	$48.7 \pm 10.4$
99.2	$15.0 \pm 0.9$	$2710 \pm 190$	0.57	$839.0 \pm 58.8$	$2.25 \pm 0.16$
109.6	$20.0 \pm 4.1$	$4320 \pm 1400$	0.57	$1337.5 \pm 433.4$	$1.27 \pm 0.41$

molecular weights, the scaling exponent for both viscosities is close to the Doi prediction of 3. However, at lower molecular weights, the exponent is lower. We are uncertain of the cause of the deviation of the data but do not believe that it should be attributed to flexibility effects. Theory predicts that an increase in chain flexibility causes a decrease in the effective length of the molecule.<sup>45</sup> Thus, the viscosity should be lower for a semirigid molecule than for a perfectly rigid rod. At a constant  $c/c^*$ , this flexibility effect would be evidenced as a decrease of the scaling exponent at higher molecular weights on the viscosity vs  $M$  plot, which is opposite to that observed experimentally. The viscosity enhancement, defined as the ratio of the maximum (Miesowicz) to minimum (zero-field) viscosity, ranges from 89 to 216, with higher molecular weight samples exhibiting a higher enhancement.

The rotational diffusivity was estimated from the experimentally determined Miesowicz viscosity,  $\eta_c$ , as described in the background section for  $C = 1.25$  and  $P = 1$ . The assumption of  $P = 1$  is justified since the lowest value of  $P$  expected could be estimated from molecular parameters to be 0.984. Other estimated parameters used in the calculations are summarized in Table 4. The isotropic viscosity  $\eta^*$  was estimated from  $\eta_c$  using eqs 8–14. The estimated isotropic viscosity  $\eta^*$  and rotational diffusivities are presented in Table 3.

Since the Miesowicz viscosity did not depend on shear rate, the rotational diffusivity was also independent of shear rate. The effect of molecular weight on the rotational diffusivity in the nematic phase can be seen in Figure 7. A molecular weight dependence of  $M_w^{-4.95 \pm 0.29} f(M)$  was observed for the rotational diffusivity. The scaling is in good agreement with Doi theory (eq 7), which predicts  $D_r \propto M^{-5} f(M)$  for a fixed  $c/c^*$ . Because the PHIC samples had PDIs ranging from 1.41 to 1.81, possible effects of polydispersity cannot be dismissed, especially in light of the extreme sensitivity

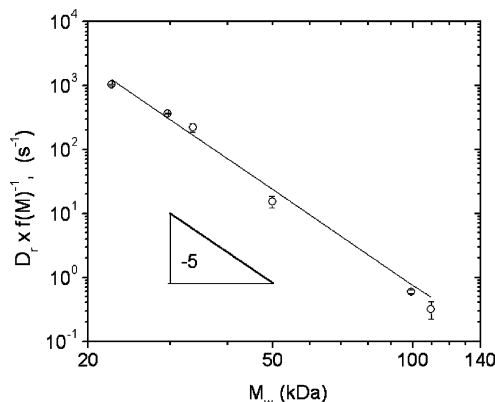
**Figure 6.** Molecular weight dependence of the transverse Miesowicz viscosity ( $\eta_c$ ) and the zero-field viscosity ( $\eta_{E=0}$ ) of PHIC solutions at  $c/c^* = 1.25$ . Both reported viscosities are weighted averages at the same range of shear rates,  $\dot{\gamma} \leq 10$   $s^{-1}$  for  $M_w \leq 33.6$  kDa and  $\dot{\gamma} \leq 1$   $s^{-1}$  for  $M_w \geq 49.8$  kDa.**Table 4. Summary of Parameters Obtained at  $C = 1.25$  and  $P = 1$** 

parameter	value	parameter	value
$S_2$	0.888	$\alpha_2/\eta^*$	-3.333
$S_4$	0.671	$\alpha_4/\eta^*$	0.127
$\lambda$	0.938	$\alpha_5/\eta^*$	3.000
$R$	0.431	$\eta_c/\eta^*$	3.230

of  $D_r$  to molecular weight. The rotational diffusivity in a polydisperse sample is expected to be affected by the high tail of the molecular weight distribution.<sup>46</sup> However, use of the other moments of the molecular weight distribution in calculating the  $M$  dependence of  $D_r$  showed similar scaling of the exponential term, i.e.,  $M_n^{-5.54 \pm 0.45}$ ,  $M_z^{-5.43 \pm 0.73}$ , and  $M_w^{-4.85 \pm 0.65}$ . This may occur because  $c^*$ , which is used to scale all calculated quantities, is determined experimentally, mitigating somewhat the impact of polydispersity on calculated values of  $D_r$ .

For design purposes, a priori prediction of properties and the rheological response is desirable and can be achieved if molecular properties, such as the rotational diffusivity, are known. We have performed these a priori estimations as follows: the infinite dilution rotational diffusivity was calculated from eq 1 using the chain dimensions of PHIC in toluene at 25 °C; the viscosity of *p*-xylene at 25 °C was taken to be 0.604 mPa·s,<sup>47</sup>  $M_w$  was used in the calculations of polymer lengths, and  $\gamma$  was calculated following the same procedure explained above. Equation 7, which assumes the phase behavior follows the Onsager relation (eq 6), was used, together with  $C = \pi \rho d L^2 / 16$  for the calculation of  $R$  and a  $\beta = 1320$ , to give a completely predictive estimate of  $D_r$ . These a priori estimates are compared in Figure 8 with the experimental values. However, the dashed line in Figure 8 shows that this completely a priori prediction overpredicts the experimental values of  $D_r$  by several orders of magnitude.

To achieve a quantitative fit, we have treated  $\beta$  as an adjustable parameter. Best agreement between

**Figure 7.** Molecular weight dependence of the rotational diffusivity calculated from plateau viscosity for PHIC at  $c/c^* = 1.25$ . Line corresponds to best fit of  $D_r [s^{-1}] \times f(M)^{-1} = 6.0 \times 10^9 M_w [kDa]^{-4.95}$ .



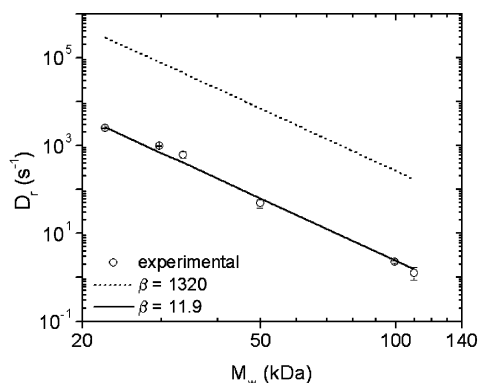


**Figure 8.** Comparison of the rotational diffusivity obtained from plateau viscosities to predictions from molecular parameters using  $\beta = 1320$  (dashed line) and a fitted  $\beta$  (solid line). Symbols correspond to experimental results, while lines correspond to predictions with eq 7, which assumes the Onsager relation.

theoretical predictions and experimental data yields  $\beta = 11.9$ . The solid line in Figure 8 shows the degree of quantitative fit using this parameter value. A  $\beta$  value of order  $10^1$  suggests that PHIC molecules in nematic solutions are much more constrained by neighbors than anticipated from simulations<sup>14</sup> and observed experimentally in semidilute solutions, where reported values are 2–5 orders of magnitude larger.

## 6. Conclusions

The rotational diffusivity of nematic solutions of rodlike polymers was extracted from experimental measurements of the transverse Miesowicz viscosity  $\eta_c$  and calculated Leslie coefficients from Doi's molecular theory without the use of decoupling approximations. Transverse Miesowicz viscosities were measured for a series of poly(*n*-hexyl isocyanate) (PHIC) polymers of  $M_w = 22.5$ –109.6 kDa at fixed dimensionless concentration ( $c/c^* = 1.25$ ) in *p*-xylene at 25 °C, by orienting the director with a high dc electric field. The rotational diffusivity of PHIC was found experimentally to be proportional to  $M_w^{-4.95 \pm 0.29} f(M)$ , verifying the prediction from Doi theory for the rotational diffusivity at a fixed  $c/c^*$  ( $D_r \propto M^{-5} f(M)$ ). Completely a priori prediction of the rotational diffusivity from molecular and solution parameters is still somewhat elusive. For PHIC the value of  $\beta$  needed for prediction from molecular parameters is of order  $10^1$ , considerably lower than reported values of order  $10^3$  or higher from simulations and experiments in semidilute solutions. At the moment, a completely a priori prediction is not possible unless a valid method for estimating  $\beta$  is developed.

**Acknowledgment.** The authors gratefully acknowledge the donors of the American Chemical Society Petroleum Research Fund (PRF-35901-AC7) and the National Science Foundation (NSF-0085026) for support of this research conducted at the University of Delaware. We thank David Thorn from DuPont for graciously supplying the catalyst.

**Supporting Information Available:** Detailed results of the molecular weight characterization with tandem SEC/light scattering; elution curves for light scattering, refractive index, and viscosity; and plots of  $Kc/R$  vs  $q^2$ , molar mass vs elution

volume,  $R_g$  vs  $M$ , and  $[\eta]$  vs  $M$ . This material is available free of charge via the Internet at <http://pubs.asc.org>.

## References and Notes

- (1) Nelson, D. S.; Soane, D. S. *Polym. Eng. Sci.* **1993**, *33*, 1619–1626.
- (2) Maffettone, P. L.; Grosso, M.; Friedenberg, M. C.; Fuller, G. G. *Macromolecules* **1996**, *29*, 8473–8478.
- (3) Tse, K. L.; Shine, A. D. *Macromolecules* **2000**, *33*, 3134–3141.
- (4) Russo, P. S.; Baylis, M.; Bu, Z.; Strykowski, W.; Doucet, G.; Temyanko, E.; Tipton, D. *J. Chem. Phys.* **1999**, *111*, 1746–1752.
- (5) Doi, M.; Edwards, S. F. *J. Chem. Soc., Faraday Trans. 2* **1978**, *74*, 918–932.
- (6) Doi, M.; Edwards, S. F. *The Theory of Polymer Dynamics*; Clarendon Press: Oxford, UK, 1986; pp 289–380.
- (7) Burgers, J. M. In *Selected Papers of J. M. Burgers*; Nieuwstadt, F. T. M., Steketee, J. A., Eds.; Kluwer Academic Publishers: Dordrecht, The Netherlands, 1995; pp 209–281. Originally published in *Second Report on Viscosity and Plasticity*; North-Holland: Amsterdam 1938; p 113.
- (8) Tirado, M. M.; Garcia de la Torre, J. *J. Chem. Phys.* **1980**, *73*, 1986–1993.
- (9) Yoshizaki, T.; Yamakawa, H. *J. Chem. Phys.* **1980**, *72*, 57–69.
- (10) Doi, M. *J. Polym. Sci., Part B: Polym. Phys.* **1981**, *19*, 229–243.
- (11) Onsager, L. *Ann. N.Y. Acad. Sci.* **1949**, *51*, 627–659.
- (12) Chow, A. W.; Fuller, G. G.; Wallace, D. G.; Madri, J. A. *Macromolecules* **1985**, *18*, 793–804.
- (13) Zero, K. M.; Pecora, R. *Macromolecules* **1982**, *15*, 87–93.
- (14) Teraoka, I.; Ookubo, N.; Hayakawa, R. *Phys. Rev. Lett.* **1985**, *55*, 2712–2715.
- (15) Mori, Y.; Ookubo, N.; Hayakawa, R. *J. Polym. Sci., Part B: Polym. Phys.* **1982**, *20*, 2111–2124.
- (16) Jamieson, A. M.; Southwick, J. G.; Blackwell, J. *J. Polym. Sci., Part B: Polym. Phys.* **1982**, *20*, 1513–1524.
- (17) Cush, R.; Russo, P. S.; Kucukyavuz, Z.; Bu, Z. M.; Neau, D.; Shih, D.; Kucukyavuz, S.; Ricks, H. *Macromolecules* **1997**, *30*, 4920–4926.
- (18) Keep, G. T.; Pecora, R. *Macromolecules* **1988**, *21*, 817–829.
- (19) Maguire, J. F.; McTague, J. P.; Rondelez, F. *Phys. Rev. Lett.* **1980**, *45*, 1891–1894.
- (20) Hill, D. A.; Soane, D. S. *J. Polym. Sci., Part B: Polym. Phys.* **1989**, *27*, 2295–2320.
- (21) Phalakornkul, J. K.; Gast, A. P.; Pecora, R. *Macromolecules* **1999**, *32*, 3122–3135.
- (22) Tsvetkov, V. N.; Andreeva, L. N.; Lezov, A. V.; Tsvetkov, N. V. *Eur. Polym. J.* **1990**, *26*, 163–169.
- (23) Kwon, M. H.; Lee, Y. S.; Park, O. O. *Korean J. Chem. Eng.* **1999**, *16*, 265–273.
- (24) Hirai, T.; Fujimura, N.; Urakawa, O.; Adachi, K.; Donkai, M.; Se, K. *Polymer* **2002**, *43*, 1133–1138.
- (25) Gatzonis, Y.; Siddiquee, S. R.; VanEgmond, J. W. *Macromolecules* **1997**, *30*, 7253–7262.
- (26) Immaneni, A.; McHugh, A. J. *J. Polym. Sci., Part B: Polym. Phys.* **1998**, *36*, 181–190.
- (27) Gleeson, J. T.; Larson, R. G.; Mead, D. W.; Kiss, G.; Cladis, P. E. *Liq. Cryst.* **1992**, *11*, 341–364.
- (28) Larson, R. G. *The Structure and Rheology of Complex Fluids*; Oxford University Press: New York, 1999; pp 519–532.
- (29) Marrucci, G. *Mol. Cryst. Liq. Cryst.* **1982**, *72*, 153–161.
- (30) Kuzuu, N.; Doi, M. *J. Phys. Soc. Jpn.* **1984**, *53*, 1031–1038.
- (31) Beris, A. N.; Edwards, B. J. *Thermodynamics of Flowing Systems with Internal Microstructure*; Oxford University Press: New York, 1994; pp 453–570.
- (32) DeGennes, P. G.; Prost, J. *The Physics of Liquid Crystals*, 2nd ed.; Clarendon Press: Oxford, UK, 1993.
- (33) Lee, Y. C.; Huh, J. D.; Chung, I. J. *Polym. J.* **1990**, *22*, 295–303.
- (34) Yang, I. K.; Shine, A. D. *J. Rheol.* **1992**, *36*, 1079–1104.
- (35) Kuzuu, N.; Doi, M. *J. Phys. Soc. Jpn.* **1983**, *52*, 3486–3494.
- (36) Larson, R. G. *The Structure and Rheology of Complex Fluids*; Oxford University Press: New York, 1999; pp 455–459.
- (37) Archer, L. A.; Larson, R. G. *J. Chem. Phys.* **1995**, *103*, 3108–3111.
- (38) Tse, K. L.; Shine, A. D. *J. Rheol.* **1995**, *39*, 1021–1040.
- (39) Patten, T. E.; Novak, B. M. *J. Am. Chem. Soc.* **1996**, *118*, 1906–1916.
- (40) Duda, A. *Polimery* **1998**, *43*, 135–143.
- (41) Ute, K.; Asai, T.; Fukunishi, Y.; Hatada, K. *Polym. J.* **1995**, *27*, 445–448.

- (42) Itou, T.; Chikiri, H.; Teramoto, A.; Aharoni, S. M. *Polym. J.* **1988**, *20*, 143–151.
- (43) Conio, G.; Bianchi, E.; Ciferri, A.; Krigbaum, W. R. *Macromolecules* **1984**, *17*, 856–861.
- (44) Itou, T.; Teramoto, A. *Macromolecules* **1988**, *21*, 2225–2230.
- (45) Doi, M. *J. Polym. Sci., Polym. Symp.* **1985**, 93–103.

- (46) Marrucci, G.; Grizzuti, N. *J. Polym. Sci., Polym. Lett. Ed.* **1983**, *21*, 83–86.
- (47) Viswanath, D. S.; Natarajan, G. *Data Book on the Viscosity of Liquids*; Hemisphere Pub.: New York, 1989.

MA048632J